Finite Thickness Effect of a Zone Plate on Focusing Hard X-Rays

W. B. Yun, J. Chrzas, and P. J. Viccaro

Argonne National Laboratory,
Advanced Photon Source
9700 S. Cass Ave. Argonne IL. 60439

ABSTRACT

Spatial resolution and focusing efficiency are two important properties of a zone plate in x-ray focusing applications. A general expression of the zone plate equation describing its zone registration is derived from the interference of spherical waves emited from two mutually coherent point sources. An analytical expression of the focusing efficiency in terms of the zone plate thickness and x-ray refractive indices of the zones is also derived. Validity condition for using this expression is considered. Thickness required for obtaining adequate focusing efficiency is calculated as a function of x-ray energy for several representative materials. The spatial resolution of a finite thickness zone plate is worse than that of an infinetly thin zone plate, which is approximately equal to the smallest zone width of the zone plate. The effect of the finite thickness on the spatial resolution is considered.

Focusing of electromagnetic wave by a Fresnel zone plate was demonstrated approximately 100 years ago by Soret.[1] A Fresnel zone plate consists of concentric zones with alternative optical refractive indexes. The distribution of the zones in the zone plate alters an incident wavefront in such a way that the beam emerging from the zones interferes constructively at the focus of the zone plate. The wavefront alteration is obtained by either attenuation or phase change of the incident wave by neighboring zones. The spatial resolution of the zone plate is approximately equal to its smallest zone width.

In recent years x-ray microfocusing using Fresnel zone plates as focusing elements has made significant progress.[2,3] Soft x-ray microscopy using zone plates has obtained spatial resolution better than 500Å.[2] and Living biological samples were imaged at that resolution. The zone plates were produced either by electron microscope[4] or deep UV interferometry based lithographic techniques.[5] In these techniques, a zone plate pattern is written on a high resolution electron or photon sensitive resist and the pattern is subsequently transferred lithographically into a zone plate.

A soft x-ray version of the interferometry technique was shown theoretically capable of producing high resolution zone plates by recording the interference patterns of its two different diffraction orders of coarser zone plates.[6] The lithographic process involved in these techniques, however, is limited to producing zone plates with a small aspect ratio, which is defined as the ratio of the zone plate thickness to the smallest zone width. As a consequence, the use of the high resolution zone plates made by this lithographic based technique is limited to the soft x-ray spectrum regime (wavelength longer than 10Å).

To produce zone plates with a large enough aspect ratio for hard x-ray focusing applications, a sputter slicing technique has been developed[7,8]. A zone plate produced by this technique can in fact have any designed aspect ratio. While a thick zone plate is necessary to obtain adequate focusing efficiency for hard x-ray focusing applications, the finite thickness of the zone plate also results in a decrease of the spatial resolution predicted for an infinite thin zone plate. In this work the thickness of a zone plate required for focusing x-rays of energy 0.1-100Kev is calculated, and the effect of the finite thickness of the zone plate on its spatial resolution is determined.

Hologram of Two Mutually Coherent Point Sources As A Zone Plate

The intensity distribution of the interference pattern of two spherical waves of the same frequency with fixed phase relationship emitted from point sources is well established [9]. The two point sources and their associated spherical waves are said to be mutually coherent. The intensity distribution of the interference pattern formed by a spherical wave emitting from a point source S_1 and a mutually coherent spherical wave converging to a point source (i.e., a virtual point source) S_2, see Fig. 1, is

$$I(r_1, r_2) = 2\left[1 + cos\left(k\left(r_1 + r_2\right) - \phi\right)\right] \tag{1}$$

where r_1 and r_2 are the amplitudes of the vectors r_1 and r_2, $k = 2\pi/\lambda$ is the wave number and ϕ the relative phase delay of source S_2 with respect to source S_1. In deriving this expression we have assumed that the two point sources have identical amplitudes at the point of interest. Note that the intensity distribution can also be uniquely specified by the phase of the interference field $k\left(r_1 + r_2\right) - \phi$. The interference pattern is azimuthally symmetrical about the axis passing through the point sources S_1 and S_2. It is therefore sufficient to describe the intensity distribution in a plane passing through the symmetry axis, i.e. XY plane in figure 1.

A record of the interference pattern between S_1 and S_2 on a thin planar medium (e.g. film) is a 2-dimensional hologram. Depending on the nature of the recording medium, the recorded information can be either the intensity or phase distribution of the interference field or combination of the two. The spherical wave converging to S_2 used in recording the hologram is reconstructed by illuminating the hologram with the spherical wave emerging from S_1. In the reconstruction process the hologram converts part of the incident wave into the spherical wave being reconstructed by absorption, if the intensity was recorded in the hologram, or introduction of phase change, if the phase distribution was recorded, or the combination of two. Effectively the hologram in the reconstruction process acts as a focusing device in focusing the radiation emitting from the point source S_1 to the point S_2. It is shown later in this section that the hologram is a generalized zone plate. The principle of zone plate focusing is identical to the reconstruction of the converging spherical wave by the hologram. This principle is valid for the full electromagnetic spectrum, including the the visible light spectrum regime as well as the x-ray spectrum regime.

The intensity variation given by Eq.1 between two nodes or antinodes of the interference field is a *cosine* function. It is therefore sufficient to describe the distribution of the nodes and the antinodes for describing the interference pattern. The condition for formation of the antinodes in the interference pattern is

$$k\left(r_1 + r_2\right) - \phi = 2m'\pi$$

or

$$r_1 + r_2 = m'\lambda + \frac{\lambda\phi}{2\pi}, \tag{2}$$

where $m' > 0$ is an integer. Similarly the condition for formation of the nodes is

$$r_1 + r_2 = \left(m' + 1/2\right)\lambda + \frac{\lambda\phi}{2\pi} \tag{3}$$

Eqs. (2) and Eq. (3) can be combined into one form

$$r_1 + r_2 = \left(m'' + \frac{\phi}{\pi}\right)\lambda/2, \tag{4}$$

with m'' being an integer, 1 2, 3, ... Eq. (2) and Eq. (3) are now presented with m'' being even and odd integers, respectively.

For given λ, ϕ and m'', the right hand side of Eq. (4) is a constant. The expression of Eq. (4) is then identical to the definition of an ellipse. For a given pair of λ and ϕ, Eq. (4) indicates that the antinodes and the nodes of the interference pattern form a set of ellipses, each specified by a m'' value. S_1 and S_2 are the common foci of all the ellipses. The major axis of an ellipse specified by a m'' value $2a''_m$ is

$$2a''_m = r_1 + r_2 = \left(m'' + \frac{\phi}{\pi}\right)\lambda/2. \tag{5}$$

The difference between the major axises of two neighboring ellipses, one associated with a node and the other with antinode, is $\lambda/2$. The same quantity for two neighboring ellipsoids associated with two nodes or two antinodes is equal to λ.

The condition for an ellipse to be physically allowed requires its major axis to be longer than the distance between two foci $2c$, i.e. $a_{m''} > c$ in our case (see Fig.2). The smallest m'' value m''_0 which satisfies that condition is found from Eq. (5), $m''_0 \geq 4c/\lambda - \phi/\pi$. The lower and upper limits of the half major axis of the corresponding ellipse $a_{m''_0}$ are

$$c \leq a_{m''_0} < c + \lambda/4.$$

Define $m = m'' - m''_0$. Eq. (5) can be rewritten as

$$a_m = a_0 + m\lambda/4, \tag{6}$$

where $a_0 = a_{m_0''}$. The definition $m = m'' - m_0''$ has a clear physical meaning and its value is the index of the physically allowed ellipses counted outward with $m = 0$ being the first. An increment in m by 1 represents a change from an ellipse associated with a node to the one associated with an antinode, or another way around.

Using the notation in Fig. 2, the equation of an ellipse specified by m is

$$\frac{x^2}{a_m^2} + \frac{y^2}{b_m^2} = 1,$$

where b_m is the half minor axis of the ellipse

$$b_m^2 = a_m^2 - c^2 = \Lambda + a_0 m\lambda/2 + \frac{(m\lambda)^2}{16}, \tag{7}$$

where $\Lambda = a_0^2 - c^2$. $b_0 = \sqrt{\Lambda}$ is the half minor axis of the ellipse with the half major axis a_0. The lower and upper limits of b_0 is

$$0 \le b_0 = \sqrt{\Lambda} < c\lambda/2 + \lambda^2/16.$$

The position of an ellipse specified by m along the Y axis in a plane between S_1 and S_2 (see Fig.2) is

$$y_m^2 = \left(1 - \frac{x^2}{a_m^2}\right) b_m^2 = \left(1 - \frac{(c-f)^2}{a_m^2}\right) \cdot \left(\Lambda + a_{m_0} m\lambda/2 + (m\lambda)^2/16\right), \tag{8a}$$

where $f = c - x$ is the distance between the plane of interest and S_2. Eq. (8) becomes

$$y_m^2 = \Lambda + a_{m_0} m\lambda/2 + (m\lambda)^2/16 \tag{8b}$$

for $f = c$, and

$$y_m^2 \simeq fm\lambda + (m\lambda)^2/4 + \Lambda\left(\frac{m\lambda}{c} + \frac{2f}{c}\right) \tag{8c}$$

for $f/c << 1$ and $m\lambda/c << 1$. For the latter case $a_0 \simeq c$ is used and all terms containing f/c or $m\lambda/c$ are neglected. The accuracy of Eq. (8c) is better than 1% for $f/c \le 0.1$ and $m\lambda/c \le 0.1$.

The expression of y_m^2 in Eq. (8c) for $A = 0$ is identical to that describing the zone positions of a zone plate of an infinite conjugate demagnification g, where the conjugate demagnification, g, is defined as the ratio of the distance between the source and the zone plate to that between the zone plate and the focusing plane. i.e., from fig.2, $g = (2c - f)/f$. An example of infinite conjugate demagnification is that the zone plate is illuminated by a plane wave, which is equivalent to $c = \infty$.

The dependence of y_m^2 on $m\lambda$ is identical in the Eqs. (8b) and Eq. (8c) except for their different multiplication factors. This difference and also the different multiplication factors of the $(m\lambda)^2$ term in the two expressions result from their different conjugate demagnifications. In Eq. (8a), $g = 1$ for Eq. (8b) and $g >> 1$ for Eq. (8c). Eq. (8a) is therefore a general expression of the zone plate equation. m is the zone index of the zone plate. The effective focal length of the generalized zone plate is

$$f_e = c\left(1 - \frac{(c-f)^2}{c^2}\right)/2. \tag{9}$$

$f_e \simeq f$ for $f << c$ and $f_e = c/2$ for $f = c$.

For $m\lambda << f$, the 2nd term in both Eqs. (8b) and Eq. (8c) is dominant and the two equations become identical when other terms in the two expressions are neglected. Under this condition, the positions of the zones of the zone plate is

$$y_m^2 \simeq f_e m\lambda. \tag{10}$$

The zone plate specified by Eq. (10) can be used to obtain any conjugate demagnification. According to Young[10], Eq. (10) approximates well Eqs. (8b) and Eq. (8c) without primary spherical aberration for $m \leq m_{max} = (2f_e/\lambda)^{1/2}$. The corresponding numerical aperture of the zone plate is[11]

$$N.A. \simeq y_{max}/f_e = (2\lambda/f_e)^{1/4}, \tag{11}$$

and the spatial resolution[12]

$$\Delta_y = 0.61\frac{\lambda}{N.A.} \simeq 0.61\left(f_e\lambda^3/2\right)^{1/4}. \tag{12}$$

Note that Δ_y increases much more quickly with λ than it does with f_e. Fig.3 shows Δ_y calculated using Eq. (12) as a function of λ for several f values. The figure shows that fairly high spatial resolution can be obtained from a zone plate characterized by Eq. (10) and of reasonable focal length for x-rays of energy greater than 1Kev. Thereafter in this work we assume that zone plate equation is given by Eq. (10) unless otherwise specified.

Focusing Efficiency of a Zone Plate

It is necessary that a zone plate has adequate thickness to modify the incident wave front to obtain focusing. The zone plate described by Eq. (10) has a periodicity of $2f\lambda$ in $r^2 = x^2 + y^2$ space. This fact is used to expand the transmittance function of the zone plate $t(r)$ in Fourier series of the form

$$t(r) = \sum_{N=-\infty}^{\infty} C_N \psi\left(r^2; -N/f\right), \tag{13}$$

where N = integers and

$$\psi\left(r^2; -N/f\right) = \exp\left[-jkNr^2/2f\right]$$

is the Vander Lugt function[13]. $\psi\left(r^2; -N/f\right)$ is periodic function in r^2 space and the period is $2f\lambda/N$. $\psi\left(r^2; -N/f\right)$ presents a spherical wave converging to a point distance f/N away from the zone plate, which is the Nth order focus of the zone plate. The Fourier transform coefficients C_N is

$$C_N = \frac{1}{2f\lambda}\int_0^{2f\lambda} t\left(r^2\right)\psi\left(r^2; N/f\right) dr^2. \tag{14}$$

The wavefront of an incident illumination beam is altered by the zone plate. The amplitude of the emerging wavefront $a(r)$ from the zone plate illuminated by an incident wave of amplitude $A(r)$ may also be expanded in the same form of Fourier expansion as in Eq. (13)

$$a(r) = \sum_{N=-\infty}^{\infty} C'_N \psi\left(r^2; -N/f\right). \tag{15}$$

where

$$C'_N = \frac{1}{2f\lambda} \int_0^{2f\lambda} t\left(r^2\right) A(r) \psi\left(r^2; N/f\right) dr^2. \tag{16}$$

The fraction of the incident beam intensity delivered to the Nth order focus is proportional to $|C'_N|^2$.

$C_N = C'_N$ when the incident beam is a monochromatic plane wave of unit amplitude and incident on the zone plate along its axis. Adopting the definition of focusing efficiency as percentage of incident radiation delivered to the Nth order focus of a zone plate,[14] the focusing efficiency of Nth order diffraction of the zone plate η_N is

$$\eta_N = |C_N|^2. \tag{17}$$

A special case is when $t\left(r^2\right) = cos\left(\pi r^2/f\lambda\right)$. In this case $C_N = 0$ except for $N = 0$ and $N = \pm 1$.[14] Another special case is when $t\left(r^2\right)$ is square wave function in r^2 space, i.e., the transmittance is constant within each zone and changes abruptly at the boundaries with its neighboring zones. Most x-ray zone plates produced have transmittance function close to the square wave form. $t\left(r^2\right)$ of a zone plate with square wave zone profile may be expressed as

$$t\left(r^2\right) = \exp\left(-ikd\right) \begin{cases} \exp\left[\left(i\delta_1 - \beta_1\right) kd\right], & 0 \le r^2 < f\lambda; \\ \exp\left[\left(i\delta_2 - \beta_2\right) kd\right], & f\lambda \le r^2 < 2f\lambda. \end{cases} \tag{18}$$

where d is the thickness of the zone plate, $n_1 = 1 - \delta_1 - i\beta_1$ and $n_2 = 1 - \delta_2 - \beta_2$ are the x-ray refractive indexes of two neighboring zones, respectively.

Substituting the expression of $t\left(r^2\right)$ in Eq. (18) into Eq. (14) we have

$$C_N = \frac{\Gamma_N}{2N\pi j}\left[\exp\left(kd\left(j\delta_1 - \beta_1\right)\right) - \exp\left(kd\left(j\delta_2 - \beta_2\right)\right)\right], \tag{19}$$

where

$$\Gamma_N = \left(1 - (-1)^N\right) = \begin{cases} 2, & \text{N =odd :} \\ 0, & \text{N =even.} \end{cases} \tag{20}$$

Using Eq. (17) we have

$$\eta_N = \begin{cases} \frac{1}{(N\pi)^2}\left(\gamma_1^2 + \gamma_2^2 - 2\gamma_1\gamma_2 cos\left(kd\left(\delta_2 - \delta_1\right)\right)\right), & \text{N =odd :} \\ 0, & \text{N =even.} \end{cases} \tag{21}$$

where $\gamma_1 = \exp\left(-kd\beta_1\right)$ and $\gamma_2 = \exp\left(-kd\beta_2\right)$.

Eq. (21) is a general expression of focusing efficiency of a zone plate with square wave zone profile as a function of the zone plate thickness d and the refractive indexes n_1 and n_2, which are dependent on the materials from which the zones are made and x-ray energy used.[15] Note that both the real and imaginary parts of the refractive indexes are contributing to the focusing. The contribution from the real parts of the refractive indexes results from phase alteration of the incident wave in their way passing through the zone plate. The contribution from the imaginary parts of the refractive indexes results from amplitude alteration of the incident wave by attenuation. Optimization in focusing efficiency can be obtained by selecting proper combination of n_1, n_2 and d.

For a given pair of n_1 and n_2, the thickness of a zone plate necessary to introduce adequate phase change or attenuation for focusing can be determined using Eq. (21). Two cases are considered here for simplicity. In the first case it is assumed that $\delta_1 = \delta_2 = 0$, i.e., no phase shift is considered and wave front modification is accomplished by absorption. This type of zone plate is referred as amplitude zone plate. In this case Eq. (21) becomes, for $N =$ odd integers,

$$\eta_N = \frac{1}{(N\pi)^2}\left(\gamma_1 - \gamma_2\right)^2 \tag{22a}$$

For $\beta_2 = 0$ (i.e., one material being vacuum or air) the equation above becomes

$$\eta_N = \frac{1}{(N\pi)^2}(\gamma_1 - 1)^2. \tag{22b}$$

Furthermore for $kt\beta_1 = \infty$ and thus $\gamma_1 = 0$, Eq. (22b) yields the well known focusing efficiencies of an amplitude zone plate, $\eta_N = 1/(N\pi)^2$.[14]

We now define the thickness d_a at which $\gamma_1 = 0.05$ as a measure of thickness required for obtaining adequate focusing efficiency The focusing efficiency at this thickness is 90% of that when $\gamma_1 = 0$ or $kd\beta_1 = \infty$, i.e., $\eta_N = 0.9/(N\pi)^2$. From the definition of γ_1, we have

$$d_a \simeq \frac{3}{k\beta_1} = 6D, \tag{22}$$

where $D = 1/2k\beta_1$ is the linear absorption length of the material from which the zone plate is fabricated.

In the second case the absorption is assumed to be negligible ($\beta_1 = \beta_2 = 0$) and the focusing results from the phase modulation of the incident x-ray wave by the zone plate. This type of zone plate is known as phase zone plate. In this case Eq. (21) becomes

$$\eta_N = \frac{2}{(N\pi)^2}(1 - cos(kd(\delta_2 - \delta_1))). \tag{22c}$$

The argument of the cosine function in Eq. (22c) $kd(\delta_2 - \delta_1)$ is the relative phase change of x-rays in passing through two neighboring zones in the zone plate. η_N is strongly dependent on the relative phase change (see Eq. (22c)). For a given pair of δ_1 and δ_2, the focusing efficiency η_N changes between 0 and $4/(N\pi)^2$ with d increasing. The minimum focusing efficiency $\eta_N = 0$ is obtained when $kd(\delta_2 - \delta_1) = M\pi$ with M being 0 and an even integer. The maximum focusing efficiency is obtained when $kd(\delta_2 - \delta_1) = M\pi$ with M being an odd integer. Note that maximum focusing efficiency obtainable from a phase zone plate is 4 times of that from an amplitude zone plate. The thickness of a phase plate required for obtaining the maximum focusing efficiency is

$$d_p = \frac{M\pi}{k(\delta_2 - \delta_1)} = Md_p^1, \tag{23}$$

where M is an odd integer and $d_p^1 = d_p\,(M = 1)$.

The minimum thickness of a phase plate d_0 required to obtain focusing efficiency equal to $\eta_N = 1/(N\pi)^2$, which is the maximum focusing efficiency obtainable from an amplitude zone plate, is given by $(1 - cos\,(kd_0\,(\delta_2 - \delta_1))) = 0.5$. Solution of this equation yields

$$d_0 = \frac{\pi}{3k\,(\delta_2 - \delta_1)} = \frac{d_p^1}{3}. \tag{24}$$

d_a, d_p^1 and d_0 are calculated as a function of x-ray energy for Si and Au using Eqs. (22) through Eq. (24). The results are shown in Fig. 4 and 5, respectively. Si and Au are selected as representative materials here because they are the material of choice in microstructure fabrication. From Fig.4 and 5 we see that $d_a < d_0$ is true for both materials in the x-ray energy range calculated. Therefore zone plates fabricated from Si or Au are essentially phase plates.

We have implicitly assumed in the forgoing discussion that x-ray propagation direction was not significantly altered inside the zone plate on its way passing through the zone plate. In another words, the increase of of x-ray beam size emerging from a zone due to diffraction is substantially smaller than the beam size entering the same zone. Large diffraction angle, approximately equal to λ/Δ, is obtained at the outmost zone of the zone plate, since the spatial resolution Δ is roughly equal to the smallest zone width. The validity condition of our foregoing discussion thus can be expressed as

$$\frac{d\lambda}{\Delta} << \Delta, \qquad or \qquad \Delta >> \sqrt{d\lambda}. \tag{25}$$

Fig. 3 shows $\sqrt{d_p^1\lambda}$ as a function of x-ray energy for Si and Au. This figure essentially shows the lower limit of the validity condition at which the analysis for focusing efficiency is valid. The limit to maximum numerical aperture obtainable due to the finite thickness is discussed in next section.

The Finite Thickness Effect of a Zone Plate on Its Spatial Resolution

The numerical aperture N. A. of an infinitely thin zone plate is given by Eq. (11) and the corresponding spatial resolution by Eq. (12). A zone plate of finite thickness can be viewed as a stack of infinitely thin zone plates. All the thin zone plates hava the same focal length and each contribute partially to the overall focusing. The focusing planes of any two thin zone plates do not coincide and the separation between them is the same as the separation between the two thin zone plates. Fig. 6 shows two such thin zone plates, with one located at the front surface and another at the end surface of the zone plate. Their focusing planes are also shown in that figure. The beam size at the focusing plane P_1 of the thin zone plate at the end surface of the zone plate is approximately

$$\Delta' = sin\,(\theta)\,d = N.A.d. \tag{26}$$

The increase in beam size due to the finite thickness of the zone plate is, using Eq. (12) and Eq. (26),

$$\Delta' - \Delta = \left(\frac{(N.A.)^2\,d}{\lambda} - 1\right)\Delta.$$

Setting this increase to be equal or less than $\Delta/4$, solution of the equation above yields the maximum numerical aperture obtainable from the zone plate

$$N.A. \leq \left(\frac{5\lambda}{4d}\right)^{1/2},$$

and the spatial resolution

$$\Delta' = N.A.d = \left(\frac{5}{4}d\lambda\right)^{1/2}.$$

For hard x-ray applications d in the equation above may be replaced by d_p

$$\Delta' = \left(\frac{5M}{4}d_p^1\lambda\right)^{1/2} \tag{27}$$

Fig.3 shows $\left(d_p^1\lambda\right)^{1/2}$ as a function of x-ray energy calculated for Si and Au. Δ' for $M = 1$ is $(5/4)^{1/2} = 1.18$ times of that shown in Fig.3. Note from Eq. (27) that the spatial resolution of a zone plate decreases with its thickness increasing. For a phase zone plate of thickness Md_p^1, the decrease in the spatial resolution is proportional to $\sqrt{M}$.

Summary

It is necessary that a zone plate has sufficient thickness to modify the incident wave to obtain adequate focusing efficiency. The finite thickness of a zone plate results in a decrease of the spatial resolution predicted from an infinitely thin zone plate.

1. J. L. Soret, "Concerning diffraction by circular gratings", Arch. Sci. Phys. Nat. 52, 320(1875).

2. See several articles in X-Ray Microscopy II, D. Sayre, M. Howells, J. Kirz and H. Rarback (eds), Proc. of the international Symp., Brookhaven, NY, August 31-September 4, 1987, Springer Verlag.

3. N. M. Ceglio, J. X-Ray Science and Technology, 1, 7 (1989).

4. E. H. Anderson, "Fabrication Technology and Applications of Zone Plates", in X-Ray/EUV Optics for Astronomy and Microscopy, R. B. Hoover ed., SPIE, 1160, 2 (1989).

5. G. Schmahl, D. Rudolph, P. Guttman, and O. Christ, "Zone Plates for X-Ray Micrscopy" in X-Ray Microscopy, G. Schmahl and D. Rudolph (eds.), Springer Series in Optical Science, 43, 63 (1984)..

6. W. B. Yun and M. R. Howells, "High resolution Fresnel zone plates for x-ray applications by spatial-frequency multiplication", J. Opt. Soc. Am. A., 1, 34 (1987).

7. R. M. Bionta, "Transmission gratings that diffract 8 kev x-rays", Appl. Phys. Lett., 51, 725 (1987).

8. K. Saitoh, K. Inagawa, K. Kohra, and K. Hayashi, "Characterization of sliced zone plates for hard x-rays", Rev. Sci. Instrum., 60, 1519 (1988).

9. Yu. I. Ostrovsky, M. M. Butusov, G. V. Ostrovskaya, Interferometry by Holography, Springer-Verlag, 1980..

10. M. Young, "Zone Plates and Their Aberrations", J. Opt. Soc. Am. 62, 8, 972 (1972).

11. Eq. 4.8.13 of Principles of Optics, M.Born and E.Wolf, Macmillan, New York, 1980.

12. Eq. 8.6.24 of Principles of Optics, M.Born and E.Wolf, Macmillan, New York, 1980.

13. A.Vander Lugt,"Operational Notation for The Analysis and Synthesis of Optical Data-Processing Systems",Proc. IEEE, 54, 8, 1055(1966).

14. J. Kirz, "Phase zone plates for x-rays and the extreme UV", J. Opt. Soc. Am., 64, 301 (1974).

15. R. W. James, The Optical Principles of The Diffraction of X-Rays, Chapter II3, Ox Bow Press, (1982).

Figure Captions:

Fig.1 Schematic illustration of interference of two spherical waves: one emerging from the point source S_1, and second converging to the point S_2.

Fig.2 The antinodes and the nodes of the interference of two spherical waves form a set of ellipses. The distribution of the antinodes and the nodes in a plane perpendicular to the axsis conecting the two point sources gives the expression of a generalized zone plate.

Fig.3 Spatial resolution obtainable from a zone plate specified by Eq. (10) as a function of x-ray energy calculated for several f values (solid line). The f values are labled in the figure. The doted and dashed lines are the spatial resolution obtainable from a phase plate of thickness d_p^1 calculated for Si and Au, respectively.

Fig.4 d_a, d_p^1 and d_0 calculated as a function of x-ray energy for Si. $d_a < d_0$ indicates that a zone plate fabricated from Si is a phase plate.

Fig.5 The same as that in Fig.4 but for Au.

Fig.6 Schematic illustration of the effect of finite thickness zone plate on its spatial resolution.

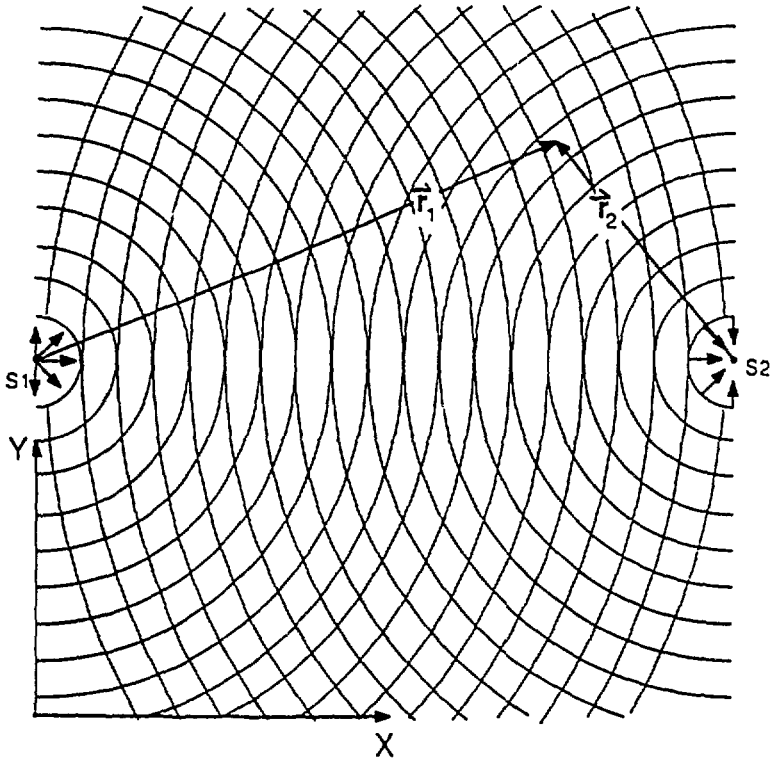

Figure 1

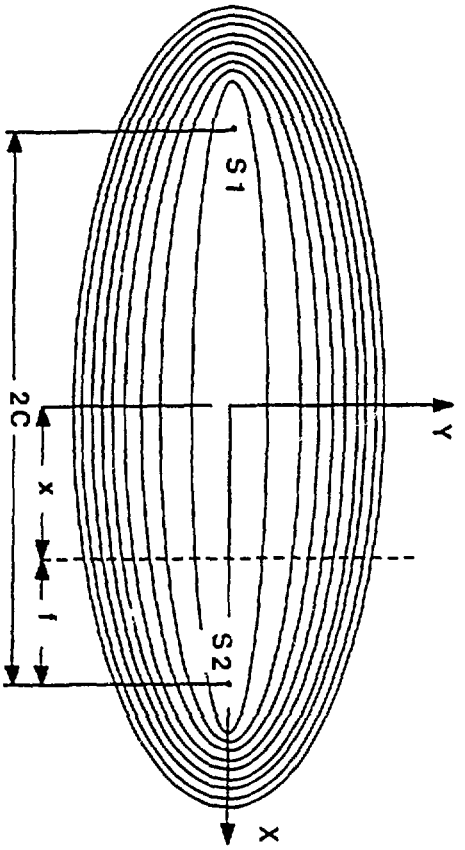

Figure 2

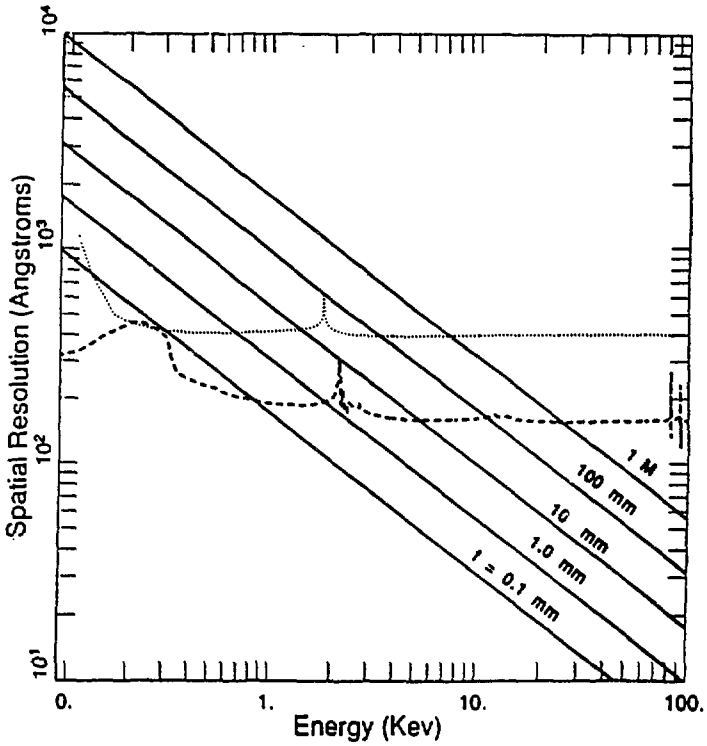

Figure 3

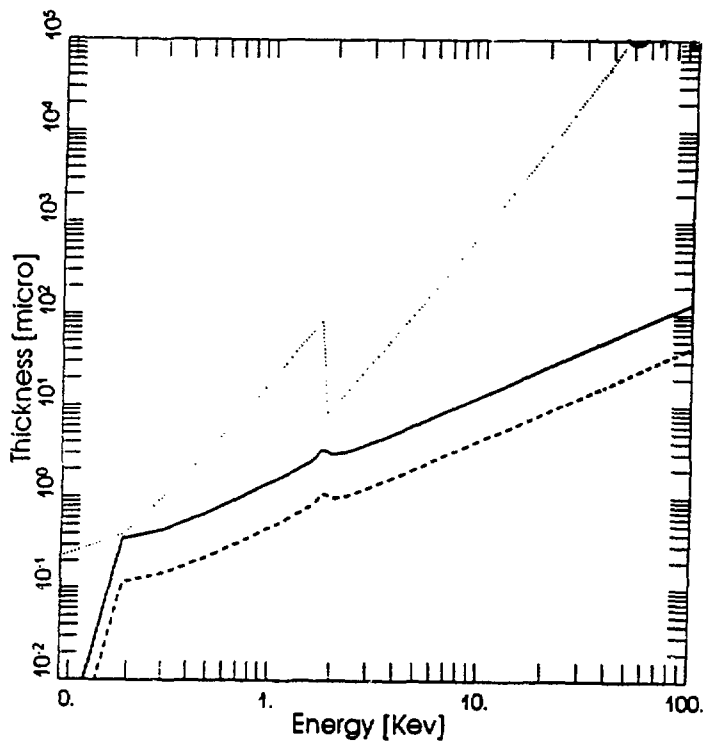

Figure 4

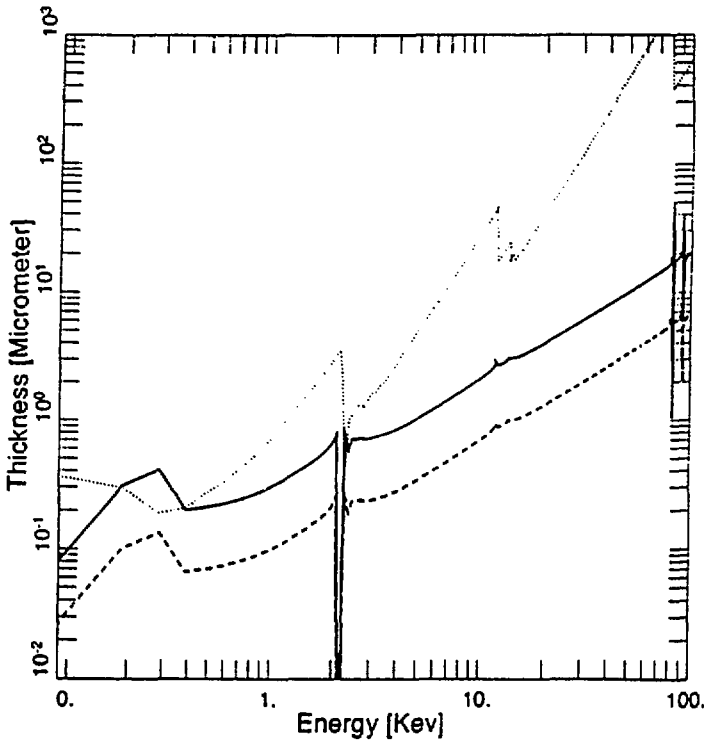

Figure 5

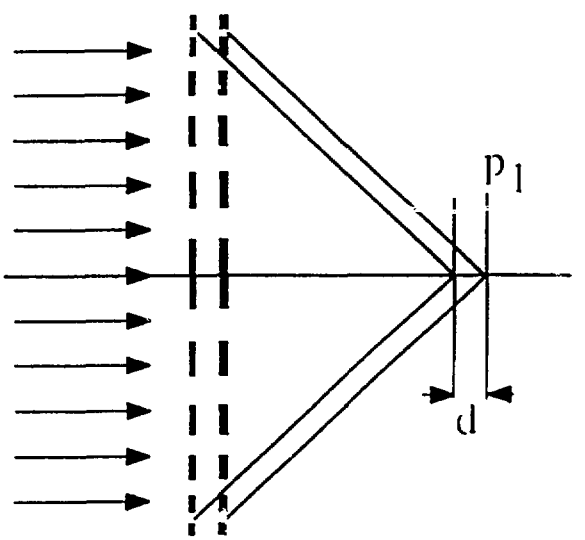

Figure 6